

## Theoretical Study of Reaction Pathways to Borazine

W. Rodger Nutt<sup>\*1a</sup> and Michael L. McKee<sup>1b</sup>*Contribution from the Departments of Chemistry, Martin Chemical Laboratory, Davidson College, Davidson, North Carolina 28035 and Auburn University, Auburn, Alabama 36849*

Received February 1, 2007

Four reaction pathways from diborane and ammonia to borazine, (HBNH)<sub>3</sub>, have been studied computationally at the density functional level (B3LYP/6-311+G(2d,p)//B3LYP/6-31G(d)). The cycloaddition of H<sub>2</sub>BNH<sub>2</sub> to 1,3-diaza-2,4-diborabuta-1,3-diene and subsequent elimination of two molecules of H<sub>2</sub> was found to be the lowest-energy pathway to (HBNH)<sub>3</sub>. In the other pathways, the formation and conversion of the intermediates 1,3,5-triaza-2,4,6-triborahexatriene, cyclotriborazane, and 1,3,5-triaza-2,4,6-triborahexa-1,5-diene into (HBNH)<sub>3</sub> were investigated. The formation of 1,3-diaza-2,4-diborabuta-1,3-diene and, subsequently, the formation and electrocyclization of 1,3,5-triaza-2,4,6-triborahexatriene and the cycloaddition of H<sub>2</sub>BNH<sub>2</sub> to 1,3-diaza-2,4-diborabuta-1,3-diene are predicted to be the kinetically favored pathways to (HBNH)<sub>3</sub> in the gas phase. At low concentrations of 1,3-diaza-2,4-diborabutene, high concentrations of H<sub>2</sub>BNH<sub>2</sub>, and a temperature of 298.15 K, the formation of the polyolefins H<sub>3</sub>BNH<sub>2</sub>(H<sub>2</sub>BNH<sub>2</sub>)<sub>n</sub>NHBH<sub>2</sub> (*n* = 1,2) is predicted to be competitive with the formation of 1,3-diaza-2,4-diborabuta-1,3-diene.

## Introduction

A gaseous mixture of diborane, B<sub>2</sub>H<sub>6</sub>, and ammonia is the preferred source for the epitaxial growth of boron nitride on a silicon substrate by chemical vapor deposition. Both compounds are available in high purity and are free of elements that could contaminate the film.<sup>2</sup> The difficulty with this source is the complexity of the chemistry and the variety of potential precursors to boron nitride. Diamminedihydroboron tetrahydroborate, [(H<sub>3</sub>N)<sub>2</sub>BH<sub>2</sub>][BH<sub>4</sub>], is formed when B<sub>2</sub>H<sub>6</sub> is condensed on liquid or solid NH<sub>3</sub>.<sup>3,4</sup> If a mixture of B<sub>2</sub>H<sub>6</sub> and NH<sub>3</sub> in a 1:2 mole ratio is heated in a sealed tube for 2–3 h at 180–190 °C, borazine, (HBNH)<sub>3</sub>, is produced in approximately 33% yield; hydrogen and an unidentified solid are isolated.<sup>3</sup> The yield of (HBNH)<sub>3</sub> can be improved by reducing the heating period and increasing the temperature.<sup>5,6</sup> Small quantities of  $\mu$ -aminodiborane, B<sub>2</sub>H<sub>5</sub>NH<sub>2</sub>, are also obtained in addition to (HBNH)<sub>3</sub>, and B<sub>2</sub>H<sub>5</sub>NH<sub>2</sub> can be prepared in yields of 33% by passing an excess of B<sub>2</sub>H<sub>6</sub> over

[(H<sub>3</sub>N)<sub>2</sub>BH<sub>2</sub>][BH<sub>4</sub>] while slowly warming the reaction tube from –130 °C to room temperature.<sup>7</sup> When gaseous B<sub>2</sub>H<sub>6</sub> and NH<sub>3</sub> are combined and allowed to pass through a pyrolysis tube that is heated from 180 to 400 °C, aminoborane, H<sub>2</sub>BNH<sub>2</sub>, is formed.<sup>8,9</sup> With the exception of B<sub>2</sub>H<sub>5</sub>NH<sub>2</sub>,<sup>10,11</sup> little is known about the reaction mechanisms that lead to these compounds or the nature of the gas-phase reactions in the deposition process.

Gómez-Aleixandre and co-workers have investigated the effect of temperature and the [B<sub>2</sub>H<sub>6</sub>]/[NH<sub>3</sub>] flow ratios on the deposition rate and composition of the BN film. They found that the turbostratic crystalline form of BN is favored when the flow ratios are low ( $\leq 0.25$ ) at 800 °C. When the flow ratios were above 0.25, amorphous films are produced. They attribute the different forms of the BN films to different precursors produced in gas-phase reactions of B<sub>2</sub>H<sub>6</sub> with NH<sub>3</sub>. Borazine is thought to be the precursor to the turbostratic form of BN. The authors point to the similarity in the arrangement of the boron and nitrogen atoms in the turbostratic form and (HBNH)<sub>3</sub> and to their detection of

\* To whom correspondence should be addressed. E-mail: ronutt@ davidson.edu.

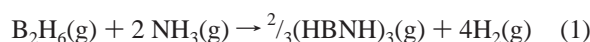
- (1) (a) Davidson College. (b) Auburn University.
- (2) (a) Rand, M. J.; Roberts, J. F. *J. Electrochem. Soc.* **1968**, *115*, 423. (b) Adams, A. C.; Capio, C. C. *J. Electrochem. Soc.* **1980**, *127*, 399.
- (3) Stock, A.; Pohland, E. *Ber.* **1926**, *59*, 2215.
- (4) Schlesinger, H. I.; Burg, A. B. *J. Am. Chem. Soc.* **1938**, *60*, 290.
- (5) Schlesinger, H. I.; Ritter, D. M.; Burg, A. B. *J. Am. Chem. Soc.* **1938**, *60*, 1296.
- (6) Wiberg, E.; Bolz, A. *Ber.* **1940**, *73*, 209.

- (7) Schlesinger, H. I.; Ritter, D. M.; Burg, A. B. *J. Am. Chem. Soc.* **1938**, *60*, 2297.
- (8) Carpenter, J. D.; Ault, B. S. *J. Phys. Chem.* **1991**, *95*, 3502.
- (9) Franz, D.; Hollenstein, M.; Hollenstein, C. *Thin Solid Films* **2000**, *379*, 37.
- (10) McKee, M. L. *J. Phys. Chem.* **1992**, *96*, 5380.
- (11) (a) Sakai, S. *J. Phys. Chem.* **1995**, *99*, 5883. (b) Sakai, S. *J. Phys. Chem.* **1995**, *99*, 9080.

(HBNH)<sub>3</sub> in the reactor as supporting evidence for their hypothesis. The amorphous BN films are rich in boron, and B<sub>2</sub>H<sub>5</sub>NH<sub>2</sub>, in which the boron to nitrogen ratio is 2:1, is the proposed precursor to this form of BN.<sup>12</sup> Clearly the ability to control the form of the BN film depends on the ability to control the formation of the appropriate precursor and, hence, a knowledge of the gas-phase chemistries.

There is a growing interest in ammineborane, H<sub>3</sub>BNH<sub>3</sub>, and ammonium tetrahydroborate, H<sub>4</sub>BNH<sub>4</sub>, as potential hydrogen storage systems.<sup>13–15</sup> The compounds have large gravimetric and volumetric densities and release H<sub>2</sub> at temperatures near 100 °C. The reaction enthalpies for the hydrogen-elimination reactions are slightly exothermic.<sup>13,15c</sup> The thermolysis of H<sub>3</sub>BNH<sub>3</sub> has been studied with the aid of differential scanning calorimetry and thermogravimetry.<sup>15</sup> Evolution of H<sub>2</sub> occurs in two exothermic steps when H<sub>3</sub>-BNH<sub>3</sub> is heated over a temperature range of 67 to 227 °C. The first step is associated with the production of 1.1 moles of H<sub>2</sub> per mole of H<sub>3</sub>BNH<sub>3</sub>. In the second step, gaseous H<sub>2</sub>-BNH<sub>2</sub> and (HBNH)<sub>3</sub> are formed along with H<sub>2</sub>. Unfortunately, (HBNH)<sub>3</sub> is an unwanted contaminant in the hydrogen feed to a fuel cell.<sup>14</sup> Knowledge of possible reaction pathways to (HBNH)<sub>3</sub> would aid the development of a process such as nanoscaffold mediation<sup>14</sup> that minimizes the formation of (HBNH)<sub>3</sub>.

We have initiated a theoretical study of reaction pathways from diborane and ammonia to borazine (eq 1) in the gas phase. The change in enthalpy for the overall reaction (eq



1) is  $-69.1$  kcal/mol.<sup>16</sup> This system provides a unique opportunity to investigate both hydrogen-elimination and condensation reactions, to identify aminoborane or ammineborane intermediates with sufficient stability to serve as precursors and to elucidate the minimum-energy pathway to borazine.

## Computational Methods

The *Gaussian 98*<sup>17</sup> program was used for all of the calculations. The geometries of the minima and transition-state structures were optimized at the B3LYP/6-31G(d) level. The nature of the stationary points associated with these structures was determined using a vibrational analysis at the same level. Local minima connected to the transition states were found with the aid of intrinsic reaction coordinate calculations at the B3LYP/6-31G(d) level. All of the

enthalpy values in the text were calculated at B3LYP/6-311+G-(2d,p)//B3LYP/6-31G(d) + ZPE and 298.15 K, if not specifically stated. Single-point energies at B3LYP/6-311+G(2d,p)//B3LYP/6-31G(d) and B3LYP/6-31G(d) levels, zero-point energies (kcal/mol), thermal corrections, and entropies at B3LYP/6-31G(d) level are reported in the Supporting Information (Table S1).

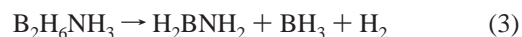
## Results and Discussion

Matrix-isolation infrared spectrophotometry has been used to study the gas-phase reaction of B<sub>2</sub>H<sub>6</sub> with NH<sub>3</sub>. Gaseous mixtures of B<sub>2</sub>H<sub>6</sub> in argon or N<sub>2</sub> and NH<sub>3</sub> in argon or N<sub>2</sub> were combined and allowed to pass through a pyrolysis zone, prior to the deposition of the reaction mixture on a cold window. Infrared bands associated with H<sub>2</sub>BNH<sub>2</sub> appeared when the temperature of the pyrolysis zone was 180 °C. The intensity of the bands increased, and the intensities of the B<sub>2</sub>H<sub>6</sub> and NH<sub>3</sub> bands decreased as the temperature of the pyrolysis zone increased to 360 °C. The results were unaffected by the variation of the B<sub>2</sub>H<sub>6</sub>/NH<sub>3</sub> ratio from 1:2 to 2:1.<sup>8</sup>

Two theoretical studies have identified the formation of amminediborane, B<sub>2</sub>H<sub>6</sub>NH<sub>3</sub> (**1**), as the first step (eq 2) in the reaction pathway from B<sub>2</sub>H<sub>6</sub> and NH<sub>3</sub> to H<sub>2</sub>BNH<sub>2</sub>. McKee reported an energy barrier ( $\Delta H(0 \text{ K})$ ) of 12.8 kcal/mol at MP4/6-31+G(2d,p)//MP2/6-31G(d) + ZPE.<sup>10</sup>



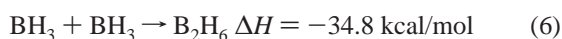
Sakai found a lower energy pathway, for which the barrier is 5.4 kcal/mol at MP4/6-311+G(d,p)//MP2/6-31G(d,p) + ZPE, and the transition state (**TS1**) has C<sub>s</sub> symmetry.<sup>11a</sup> When the latter pathway is modeled at the B3LYP/6-31G(d) level, both the transition state and **1** have C<sub>s</sub> symmetry, and the barrier for the reaction is 7.4 kcal/mol at B3LYP/6-311+G-(2d,p)//B3LYP/6-31G(d) + ZPE. The minimum-energy pathway from the B<sub>2</sub>H<sub>6</sub>NH<sub>3</sub> to H<sub>2</sub>BNH<sub>2</sub> is the 1,3-hydrogen elimination reaction (eq 3).<sup>11a</sup> The barrier (**TS2**) for this step is 23.7 kcal/mol at MP4/6-311+G(d,p)//MP2/6-31G(d,p) + ZPE,<sup>11a</sup> 23.6 kcal/mol at CCSD(T)/CBS + ZPE,<sup>18</sup> and 20.2 kcal/mol at B3LYP/6-311+G(2d,p)//B3LYP/6-31G(d) + ZPE.



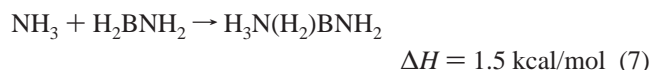
There are three possible outcomes for the borane, BH<sub>3</sub>. BH<sub>3</sub> may combine with H<sub>2</sub>BNH<sub>2</sub> to form B<sub>2</sub>H<sub>5</sub>NH<sub>2</sub> (eq 4),<sup>11a</sup> with NH<sub>3</sub> to produce H<sub>3</sub>BNH<sub>3</sub> (eq 5), or with a second BH<sub>3</sub> to obtain B<sub>2</sub>H<sub>6</sub> (eq 6). Calculations at the B3LYP/6-311+G-

- (12) (a) Gómez-Aleixandre, C.; Díaz, D.; Orgaz, F.; Albella, J. M. *J. Phys. Chem.* **1993**, *97*, 11043. (b) Gómez-Aleixandre, C.; Essafiti, A.; Fernández, M.; Fierro, J. L. G.; Albella, J. M. *J. Phys. Chem.* **1996**, *100*, 2148.
- (13) Dixon, D. A.; Gutowski, M. *J. Phys. Chem. A* **2005**, *109*, 5129.
- (14) Gutowska, A.; Li, L.; Shin, Y.; Wang, C. M.; Li, X. S.; Linehan, J. C.; Smith, R. S.; Kay, B. D.; Schmid, B.; Shaw, W.; Gutowski, M.; Autrey, T. *Angew. Chem., Int. Ed.* **2005**, *44*, 3578.
- (15) (a) Baumann, J.; Baitalov, F.; Wolf, G. *Thermochim. Acta* **2005**, *430*, 9. (b) Baitalov, F.; Baumann, J.; Wolf, G.; Jaenicke-Rössler, K.; Leitner, G. *Thermochim. Acta* **2002**, *391*, 159. (c) Wolf, G.; Baumann, J.; Baitalov, F.; Hoffmann, F. P. *Thermochim. Acta* **2000**, *343*, 19.
- (16) Calculated from the heats of formation found in: Linstrom, P. J.; Mallard, W. G. Eds. *NIST Chemistry WebBook* [Online]; NIST Standard Reference Database Number 69, June 2005; National Institute of Standards and Technology: Gaithersburg, MD. <http://webbook.nist.gov/chemistry/>.

- (17) Frisch, M. J.; Trucks, G. W.; Schlegel, H. B.; Scuseria, G. E.; Robb, M. A.; Cheeseman, J. R.; Zakrzewski, V. G.; Montgomery, J. A., Jr.; Stratmann, R. E.; Burant, J. C.; Dapprich, S.; Millam, J. M.; Daniels, A. D.; Kudin, K. N.; Strain, M. C.; Farkas, O.; Tomasi, J.; Barone, V.; Cossi, M.; Cammi, R.; Mennucci, B.; Pomelli, C.; Adamo, C.; Clifford, S.; Ochterski, J.; Petersson, G. A.; Ayala, P. Y.; Cui, Q.; Morokuma, K.; Malick, D. K.; Rabuck, A. D.; Raghavachari, K.; Foresman, J. B.; Cioslowski, J.; Ortiz, J. V.; Stefanov, B. B.; Liu, G.; Liashenko, A.; Piskorz, P.; Komaromi, I.; Gomperts, R.; Martin, R. L.; Fox, D. J.; Keith, T.; Al-Laham, M. A.; Peng, C. Y.; Nanayakkara, A.; Gonzalez, C.; Challacombe, M.; Gill, P. M. W.; Johnson, B. G.; Chen, W.; Wong, M. W.; Andres, J. L.; Head-Gordon, M.; Replogle, E. S.; Pople, J. A. *Gaussian 98*; Gaussian, Inc.: Pittsburgh, PA, 1998.
- (18) Nguyen, M. T.; Nguyen, V. S.; Matus, M. H.; Gopakumar, G.; Dixon, D. A. *J. Phys. Chem. A* **2007**, *111*, 679.

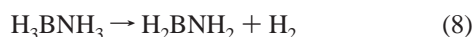


(2d,p)//B3LYP/6-31G(d) level indicate that all three reactions are exothermic, have negative free energies (Table 1), and do not have energy barriers. At the CCSD(T)/CBS level, the calculated enthalpy change for eq 5 is  $-27.6$  kcal/mol.<sup>18</sup>  $\text{H}_2\text{-BNH}_2$  may also form an adduct (**2**) with  $\text{NH}_3$  (eq 7). This reaction is endothermic and has a positive free-energy and an enthalpy barrier (**TS3**) of  $0.8$  kcal/mol. The barrier height ( $\Delta H(298 \text{ K})$ ), when compared with the enthalpy change for eq 7, is unrealistic and, hence, transition state **TS3** is not well characterized at the B3LYP/6-311+G(2d,p)//B3LYP/



6-31G(d) level. The distance between the ammonia nitrogen atom and the boron atom in **TS3** is  $2.777 \text{ \AA}$  at this level. When **TS3** is optimized at the B3LYP/6-311+G(2d,p) level, the B–N distance decreases to  $2.182 \text{ \AA}$ , and the enthalpy barrier to **2** increases to  $1.9$  kcal/mol. The formation of **2** is less favorable than the formation of  $\text{B}_2\text{H}_5\text{NH}_2$ ,  $\text{H}_3\text{BNH}_3$ , or  $\text{B}_2\text{H}_6$ , and  $\text{B}_2\text{H}_6$  is more stable than  $\text{B}_2\text{H}_5\text{NH}_2$  or  $\text{H}_3\text{BNH}_3$ .

Carpenter and Ault have investigated<sup>19</sup> the pyrolysis of gaseous  $\text{H}_3\text{BNH}_3$  with matrix-isolation infrared spectrophotometry. Infrared bands associated with  $\text{H}_2\text{BNH}_2$  were observed at  $65 \text{ }^\circ\text{C}$ . As the temperature of the pyrolysis zone was increased to  $300 \text{ }^\circ\text{C}$ , the intensity of these bands increased, and the intensity of the bands associated with  $\text{H}_3\text{-BNH}_3$  decreased. Small amounts of  $\text{NH}_3$  and  $\text{B}_2\text{H}_6$  were also detected.<sup>19</sup> The unimolecular elimination of  $\text{H}_2$  from  $\text{H}_3\text{BNH}_3$  (eq 8) is one possible path to the aminoborane. The calculated energy barrier (**TS4**,  $\Delta H(0 \text{ K})$ ) for this reaction is  $37.9$  kcal/mol at MP4/6-31+G(2d,p)//MP2/6-31G(d) + ZPE,<sup>10</sup>  $37.5$  kcal/mol at MP4/6-311+G(d,p)//MP2/6-31G(d,p) + ZPE,<sup>11a</sup>  $36.2$  kcal/mol at CCSD(T)/CBS + ZPE,<sup>18</sup> and  $34.3$  kcal/mol at B3LYP/6-311+G(2d,p)//B3LYP/6-31G(d) + ZPE.



There is an alternative route to  $\text{H}_2\text{BNH}_2$  that involves the formation of  $\text{B}_2\text{H}_6\text{NH}_3$  from  $\text{H}_3\text{BNH}_3$  (eq 9) and, subsequently, the elimination of  $\text{H}_2$  from  $\text{B}_2\text{H}_6\text{NH}_3$  (eq 3). The energy barrier (**TS5**,  $\Delta H(0 \text{ K})$ ) for the first step (eq 9) of



this path is  $13.9$  kcal/mol. Because the energy barrier for the unimolecular elimination of  $\text{H}_2$  from  $\text{H}_3\text{BNH}_3$  (eq 8) is  $14.1$  kcal/mol higher than the barrier for the elimination of  $\text{H}_2$  from  $\text{B}_2\text{H}_6\text{NH}_3$  (eq 3), the alternative route is the more favorable path from  $\text{H}_3\text{BNH}_3$  to  $\text{H}_2\text{BNH}_2$ . The free-energy barrier for **TS5** ( $21.0$  kcal/mol) increases with an increase in temperature, and the barrier heights of the hydrogen-elimination reactions (eqs 3 and 8) vary only slightly with a

**Table 1.** Reaction Enthalpies and Free Energies (kcal/mol) at the B3LYP/6-311+G(2d,p)//B3LYP/6-31G(d) Level and  $298.15 \text{ K}$

eq		TS			reaction	
		$\Delta H(\text{OK})$	$\Delta H$	$\Delta G$	$\Delta H$	$\Delta G$
2	$\text{B}_2\text{H}_6 + \text{NH}_3 \rightarrow \text{TS1} \rightarrow \mathbf{1}$	7.4	6.5	15.3	-5.2	3.4
3	$\mathbf{1} \rightarrow \text{TS2} \rightarrow \text{H}_2\text{BNH}_2 + \text{H}_2 + \text{BH}_3$	20.2	19.8	20.8	7.0	-10.4
4	$\text{BH}_3 + \text{H}_2\text{BNH}_2 \rightarrow \text{B}_2\text{H}_5\text{NH}_2 (\mathbf{A1})$				-24.9	-13.5
5	$\text{BH}_3 + \text{NH}_3 \rightarrow \text{H}_3\text{BNH}_3$				-25.0	-15.0
6	$2\text{BH}_3 \rightarrow \text{B}_2\text{H}_6$				-34.8	-24.5
7	$\text{NH}_3 + \text{H}_2\text{BNH}_2 \rightarrow \text{TS3} \rightarrow \mathbf{2}$	1.0	0.8 <sup>a</sup>	6.8	1.5 <sup>a</sup>	11.1
8	$\text{H}_3\text{BNH}_3 \rightarrow \text{TS4} \rightarrow \text{H}_2\text{BNH}_2 + \text{H}_2$	34.3	34.2	33.8	-8.0	-16.5
9	$2\text{H}_3\text{BNH}_3 \rightarrow \text{TS5} \rightarrow \mathbf{1} + \text{NH}_3$	13.9	14.4	21.0	10.0	8.8

<sup>a</sup> See text.

variation in temperature. At  $573.15 \text{ K}$ , eq 8 has a calculated free-energy barrier that is  $6.9$  kcal/mol higher than the free-energy barrier for **TS5** ( $26.6$  kcal/mol), in the alternative pathway.

Ammonia combines with  $\mu$ -aminodiborane at  $-80 \text{ }^\circ\text{C}$  to form a stable white solid, which on heating to  $200 \text{ }^\circ\text{C}$  produces  $(\text{HBNH})_3$  in a 45% yield.<sup>7</sup> The first step in the reaction pathway from  $\text{B}_2\text{H}_5\text{NH}_2$  to  $(\text{HBNH})_3$  may be the formation of  $\text{H}_2\text{BNH}_2$  from  $\text{B}_2\text{H}_5\text{NH}_2$  and  $\text{NH}_3$ . There are three possible pathways to  $\text{H}_2\text{BNH}_2$ . In transition-state structure **TSA1**,  $\text{NH}_3$  approaches a boron atom along a line nearly colinear with a B–N bond in the  $\text{B}_2\text{H}_5\text{NH}_2$ , and the products  $\text{H}_3\text{BNH}_3$  and  $\text{H}_2\text{BNH}_2$  form (Figure 1). The calculated enthalpy barrier ( $\Delta H(298 \text{ K})$ ) to **TSA1** is  $20.0$  kcal/mol (Table 2). If the line of approach of  $\text{NH}_3$  in the transition-state structure is at an angle of  $123.4^\circ$  to the B–N bond, then only a B–H<sub>bridging</sub> bond is broken, and the product is the cis (anti) conformer of 1,3-diaza-2,4-diborabutane (**A2**). The enthalpy barrier (**TSA2**) for this step is  $17.1$  kcal/mol. **A2** can undergo a 1,4-hydrogen elimination reaction through **TSA3** ( $24.2$  kcal/mol) to form  $\text{H}_2\text{BNH}_2$ . In the third pathway,  $\text{NH}_3$  lies along a line nearly colinear with a B–H<sub>bridging</sub> bond in the transition state (**TSA4**), and the enthalpy barrier to the formation of the trans (eclipsed) conformer (**A3**) of 1,3-diaza-2,4-diborabutane is  $9.9$  kcal/mol. The classical energy barrier to the conformational isomerization of **A2** into **A3** is  $13.3$  kcal/mol and is larger than the value ( $7$  kcal/mol) at the MP2/6-31G(2d)//PBE0/6-31G(2d) level previously reported.<sup>20</sup> **A2** is predicted to be more stable than **A3** by  $11.2$  kcal/mol at the B3LYP/6-311+G(2d,p)//B3LYP/6-31G(d) level and  $12.3$  kcal/mol at the CCSD(T)/CBS level.<sup>21</sup>

The free energies of transition states **TSA1**, **TSA2**, and **TSA4** increase with an increase in temperature, and the free energy of **TSA3** decreases slightly. At  $298.15 \text{ K}$ , the free-energy barrier (**TSA1**) to  $\text{H}_2\text{BNH}_2$  and  $\text{H}_3\text{BNH}_3$  is at least  $3.3$  kcal/mol higher than the barrier (**TSA2**) to **A2** and  $8.7$  kcal/mol higher to the barrier (**TSA4**) to **A3** (Table 2). At  $573.15 \text{ K}$ , the calculated barrier heights of **TSA1**, **TSA2**, **TSA3**, and **TSA4** are  $32.1$ ,  $28.4$ ,  $22.2$ , and  $24.9$  kcal/mol, respectively. The third pathway,  $\mathbf{A1} + \text{NH}_3 \rightarrow \text{TS4} \rightarrow \mathbf{A3} \rightarrow \text{TS5} \rightarrow \mathbf{A2} \rightarrow \text{TS3} \rightarrow 2 \text{ H}_2\text{BNH}_2$ , is favored at both temperatures.

(20) Jacquemin, D.; Perpète, E. A.; Wathelet, V.; André, J. J. *Phys. Chem.* **2004**, *108*, 9616.

(21) Matus, M. H.; Anderson, K. D.; Camaioni, D. M.; Autrey, S. T.; Dixon, D. A. *J. Phys. Chem. A* **2007**, *111*, 4411.

(19) Carpenter, J. D.; Ault, B. S. *Chem. Phys. Lett.* **1992**, *197*, 171.

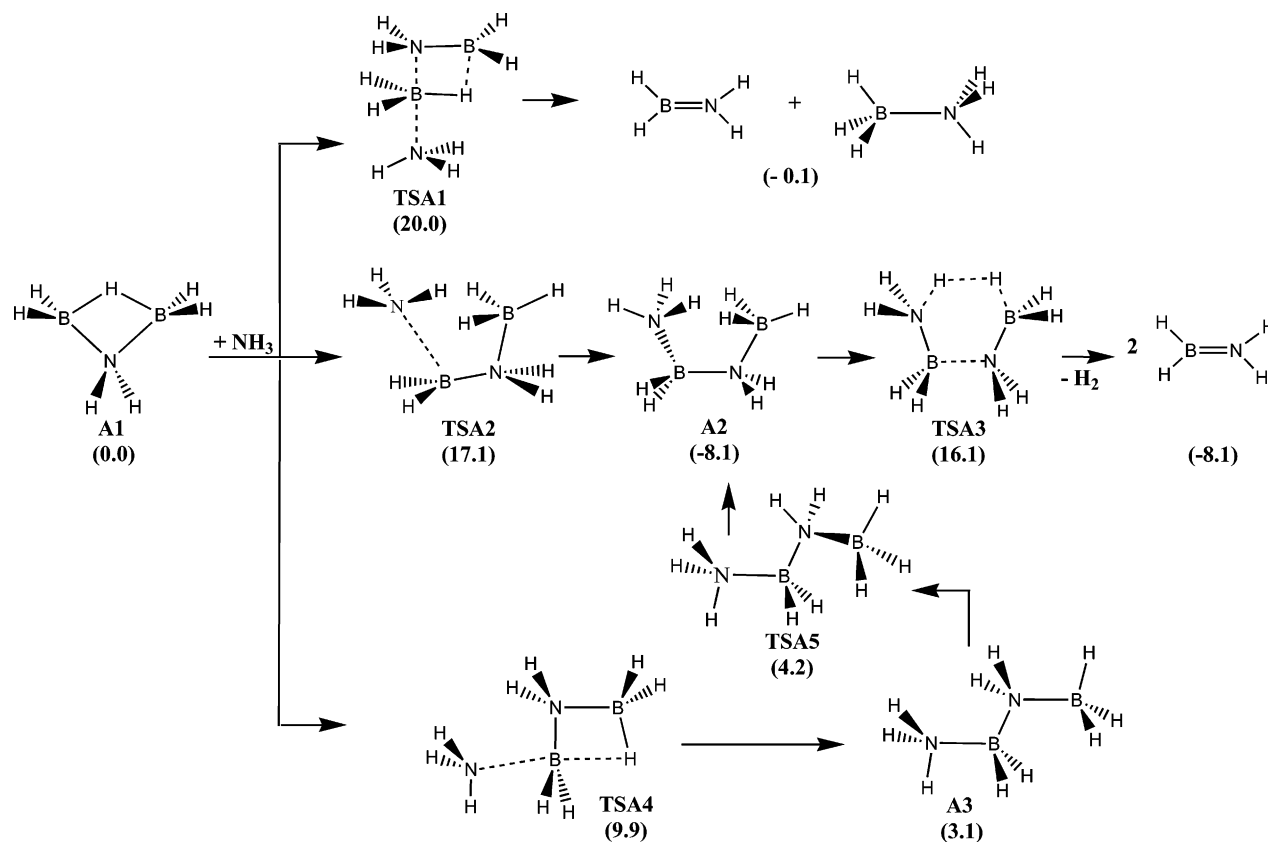


**Figure 1.** Potential-energy surface for the reaction of H<sub>2</sub>NB<sub>2</sub>H<sub>5</sub> + NH<sub>3</sub>. Enthalpies (kcal/mol) are relative to H<sub>2</sub>NB<sub>2</sub>H<sub>5</sub> + NH<sub>3</sub> at 298.15 K.

**Table 2.** Relative Enthalpies (kcal/mol) and Free Energies (kcal/mol) at the B3LYP/6-311+G(2d,p)//B3LYP/6-31G(d) Level and 298.15 K

	$\Delta H$	$\Delta G$
A1 + NH <sub>3</sub>	0.0	0.0
TSA1	20.0	26.5
TSA2	17.1	23.2
A2	-8.1	1.6
TSA3	16.1	24.9
TSA4	9.9	17.8
A3	3.1	12.0
TSA5	4.2	14.4
H <sub>2</sub> BNH <sub>2</sub> + H <sub>3</sub> BNH <sub>3</sub>	-0.1	-1.5
2 H <sub>2</sub> BNH <sub>2</sub> + H <sub>2</sub>	-8.1	-18.0

Unlike *n*-butane<sup>22</sup> the cis conformer (**A2**) of 1,3-diaza-2,4-diborabutane is more stable than the trans conformer (**A3**). The difference in energies ( $\Delta H(0\text{ K})$ ) of the conformers is 10.9 kcal/mol at B3LYP/6-311+G(2d,p)//B3LYP/6-31G(d) and 5.7 kcal/mol at MP2/6-31G(2d)//PBE0/6-31G(2d) + ZPE.<sup>20</sup> The relatively short N(1)–H···H–B(4) distance of 1.925 Å in **A2** is indicative of a dihydrogen or proton–hydride bond. This value falls in the range of intermolecular dihydrogen bond distances (1.7–2.4 Å) found in a variety of boron–nitrogen compounds<sup>23,24</sup> and is close to the recently

reported intramolecular dihydrogen bond distance of 1.95 Å.<sup>23a</sup> The formation of a dihydrogen bond contributes to the stability of **A2**. In an early theoretical study of the [H<sub>3</sub>BNH<sub>3</sub>]<sub>2</sub> complex, the average energy of an intermolecular dihydrogen bond was calculated to be 3.8 kcal/mol.<sup>24a</sup> The current predicted values are 3.2<sup>24b</sup> and 3.5<sup>24c</sup> kcal/mol for the [H<sub>3</sub>BNH<sub>3</sub>]<sub>2</sub> complex in the gas phase and 3.0 kcal/mol<sup>24d</sup> in the solid state.

**Cycloaddition Pathway.** The next logical step in the pathway to (HBNH)<sub>3</sub> is the formation of linear ammineboranes and aminoboranes. The species [H<sub>2</sub>CH<sub>3</sub>NBH<sub>2</sub>NHCH<sub>3</sub>-BH<sub>2</sub>NH<sub>2</sub>CH<sub>3</sub>][Cl] has been identified as an intermediate in the synthesis of [HBNCH<sub>3</sub>]<sub>3</sub> and [H<sub>2</sub>BNHCH<sub>3</sub>]<sub>3</sub> from [H<sub>2</sub>B(NH<sub>2</sub>CH<sub>3</sub>)<sub>2</sub>][Cl] and H<sub>3</sub>BNH<sub>2</sub>CH<sub>3</sub>.<sup>25</sup> Recently, resonances associated with polyamineboranes and polyaminoboranes were observed in the <sup>11</sup>B NMR spectra of residues that were extracted from the thermolysis of H<sub>3</sub>BNH<sub>3</sub> at 85 °C in 1-butyl-3-methylimidazolium chloride,<sup>26</sup> and strong Lewis and Brønsted–Lowry acids were found to induce dehydrogenation and polymerization of H<sub>3</sub>BNH<sub>3</sub>.<sup>27</sup>

Olefin-insertion and hydrogen-elimination reactions are the most likely paths to the linear intermediates (Figure 2). The enthalpy barrier (**TSB1**, 11.4 kcal/mol) to the formation of 1,3-diaza-2,4-diborabutene (**B1**) by the insertion of H<sub>2</sub>BNH<sub>2</sub> into the H–B bond of a second H<sub>2</sub>BNH<sub>2</sub> is relatively small

(22) Smith, G. D.; Jaffe, R. L. *J. Phys. Chem.* **1996**, *100*, 18718.

(23) (a) Jaska, C. A.; Lough, A. J.; Manners, I. *Inorg. Chem.* **2004**, *43*, 1090. (b) Jaska, C. A.; Temple, K.; Lough, A. J.; Manners, I. *J. Am. Chem. Soc.* **2003**, *125*, 9424. (c) Klooster, W. T.; Koetzle, T. F.; Siegbahn, P. E. M.; Richardson, T. B.; Crabtree, R. H. *J. Am. Chem. Soc.* **1999**, *121*, 6337. (d) Richardson, T. B.; de Gala, S.; Crabtree, R. H.; Siegbahn, P. E. M. *J. Am. Chem. Soc.* **1995**, *117*, 12875.

(24) (a) Cramer, C. J.; Gladfelter, W. L. *Inorg. Chem.* **1997**, *36*, 5358. (b) Li, J.; Zhao, F.; Jing, F. *J. Chem. Phys.* **2002**, *116*, 25. (c) Kar, T.; Scheiner, S. *J. Chem. Phys.* **2003**, *119*, 1473. (d) Morrison, C. A.; Siddick, M. M. *Angew. Chem., Int. Ed.* **2004**, *43*, 4780.

(25) (a) Beachley, O. T., Jr. *Inorg. Chem.* **1968**, *7*, 701. (b) Beachley, O. T., Jr. *Inorg. Chem.* **1967**, *6*, 870.

(26) Bluhm, M. E.; Bradley, M. G.; Butterick, R., III.; Kusari, U.; Sneddon, L. G. *J. Am. Chem. Soc.* **2006**, *128*, 7748.

(27) Stephens, F. H.; Baker, R. T.; Matus, M. H.; Grant, D. J.; Dixon, D. A. *Angew. Chem., Int. Ed.* **2006**, *45*, 1.

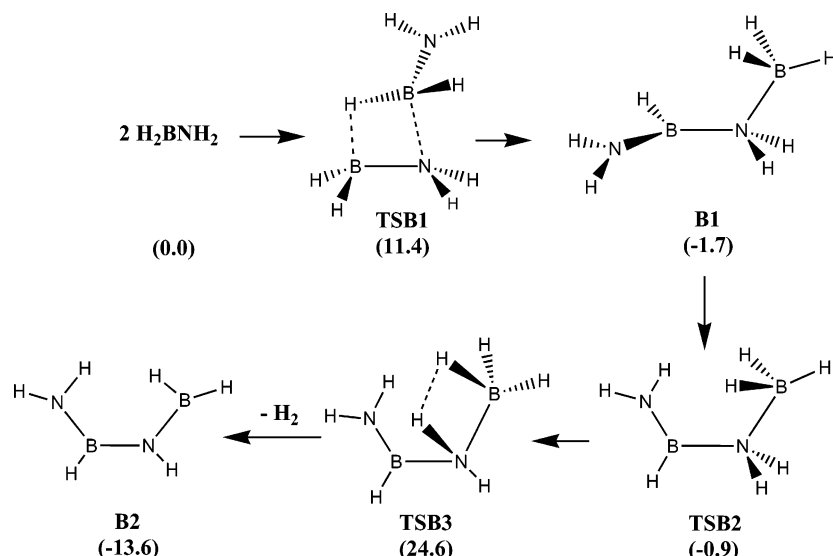


**Figure 2.** Potential-energy surface for the reaction of two  $\text{H}_2\text{BNH}_2$ . Enthalpies (kcal/mol) are relative to two  $\text{H}_2\text{BNH}_2$  at 298.15 K.

**Table 3.** Relative Enthalpies (kcal/mol) and Free Energies (kcal/mol) at the B3LYP/6-311+G(2d,p)//B3LYP/6-31G(d) Level and 298.15 K

	$\Delta H$	$\Delta G$
2 $\text{H}_2\text{BNH}_2$	0.0	0.0
<b>TSB1</b>	11.4	22.2
<b>B1</b>	-1.7	8.7
<b>TSB2</b>	-0.9	10.8
<b>TSB3</b>	24.6	35.8
<b>B2</b> + $\text{H}_2$	-13.6	-11.3

(Table 3). The unimolecular elimination of  $\text{H}_2$  by **B1** has a larger enthalpy barrier (**TSB3**, 26.3 kcal/mol) and leads to the cis isomer of 1,3-diaza-2,4-diborabuta-1,3-diene (**B2**). **TSB2** is the optimized structure obtained from the final point of the intrinsic reaction coordinate calculation in the forward direction from **TSB1** and is the transition state for rotation about the central B–N bond in **B1**. The free-energy barrier heights of **TSB1** and **TSB3** (from **B1**) are 22.2 and 27.1 kcal/mol at 298.15 K and 32.0 and 27.9 kcal/mol at 573.15 K, respectively.

The cycloaddition of  $\text{H}_2\text{BNH}_2$  to **B2** and the subsequent elimination of two molecules of  $\text{H}_2$  leads to  $(\text{HBNH})_3$  (Figure 3). The enthalpy barrier to the formation of 1,3,5-triaza-2,4,6-triboracyclohexene (**C1**) in a Diels–Alder type reaction is 11.3 kcal/mol (Table 4), and the energy barrier ( $\Delta H(0\text{ K})$ , 12.5 kcal/mol) to **C1** is similar in magnitude to the barrier height (10.7 kcal/mol) calculated for the dimerization of aminoborane at the B3LYP/6-31G(d) level.<sup>28</sup> The twist conformation of the triboracyclohexene (**C4**) is 2.2 kcal/mol less stable than the boat form (**C1**) and has a barrier height (**TSC6**) of 2.0 kcal/mol. By comparison, the twist form of cyclohexene was calculated at the B3LYP/6-31G(d,p) level to be 5.1 kcal/mol more stable than the boat form.<sup>29</sup> The extra stability of **C1** may be attributed in part to the B(6)–H $\cdots$ H–N(3) dihydrogen bond (2.310 Å).

There are three paths from **C1** to 1,3,5-triaza-2,4,6-triboracyclohexa-1,3-diene (**C2**). The lowest-energy path is a 1,4-hydrogen elimination reaction with a calculated en-

thalpy barrier (**TSC2**) of 24.3 kcal/mol. **TSC2** is a late transition state with N(3)–H and B(6)–H axial bond lengths of 1.548 and 1.526 Å, respectively. In the 1,2-hydrogen elimination pathways, the axial N(3)–H bond and the equatorial B(4)–H bond lengths (1.435 and 1.365 Å, respectively) in **TSC3** and the equatorial N(5)–H bond and the axial B(6)–H bond lengths (1.411 and 1.493 Å, respectively) in **TSC4** are shorter, and the enthalpy barrier heights are 37.8 and 43.6 kcal/mol, respectively. The transition state (**TSC5**) for the elimination of  $\text{H}_2$  from **C2** to form  $(\text{HBNH})_3$  (**C3**) has an enthalpy barrier of 25.1 kcal/mol. Han et al. predicted a classical barrier of 29.9 kcal/mol at B3LYP/6-311+G(2d,p),<sup>30</sup> which is 0.8 kcal/mol higher than the classical barrier calculated at the B3LYP/6-311+G(2d,p)//B3LYP/6-31G(d) level. Only the free-energy barrier for **TSC1** varies significantly with a variation in temperature. The value (23.8 kcal/mol) increases by 11.5 kcal/mol when the temperature is increased from 298.15 to 573.15 K. **C1**,<sup>31a</sup> **C2**,<sup>31a</sup> and **C3**<sup>31</sup> have been modeled at the B3LYP/6-311+G(d,p) level in previous theoretical studies of aromaticity.

**Electrocyclic Pathway.** The insertion of  $\text{H}_2\text{BNH}_2$  into the B(4)–H bond in **B2** leads to the hydrogen-bridged form of 1,3,5-triaza-2,4,6-triborahexa-1,3-diene (**D1**) (Figure 4). The calculated enthalpy barrier (**TSD1**, 10.9 kcal/mol) for this step is similar in magnitude to the calculated barrier height (11.4 kcal/mol) of **TSB1**. The nonbridging form of **D1** (**D2**) is 0.1 kcal/mol more stable (Table 5), and the enthalpy barrier to the conversion of **D1** into **D2** is 0.2 kcal/mol. The unimolecular elimination of  $\text{H}_2$  by **D2** gives the *cZt*<sup>32</sup>

(30) Han, S. S.; Kang, J. K.; Lee, H. M.; van Duin, A. C. T.; Goddard, W. W., III *J. Chem. Phys.* **2005**, *123*, 114703.

(31) (a) Phukan, A. K.; Kalagi, R. P.; Gadre, S. R.; Jemmis, E. D. *Inorg. Chem.* **2004**, *43*, 5824. (b) Kiran, B.; Phukan, A. K.; Jemmis, E. D. *Inorg. Chem.* **2001**, *40*, 3615.

(32) Z in the E–Z system indicates that the groups with higher CIP priority to the left and right of a double bond are cis to one another. The lowercase c or s cis and lowercase t or s trans specify the spatial arrangement of the double bonds on each end of a single bond. In the *cZc* conformer of hexatriene, the double bonds to the left and right of the central double have a cis orientation, and the double bonds on each end of the single bonds are cis to one another.

(28) Gilbert, T. M. *Organometallics* **1998**, *17*, 5513.

(29) Kraka, E.; Wu, A.; Cremer, D. *J. Phys. Chem. A* **2003**, *107*, 9008.

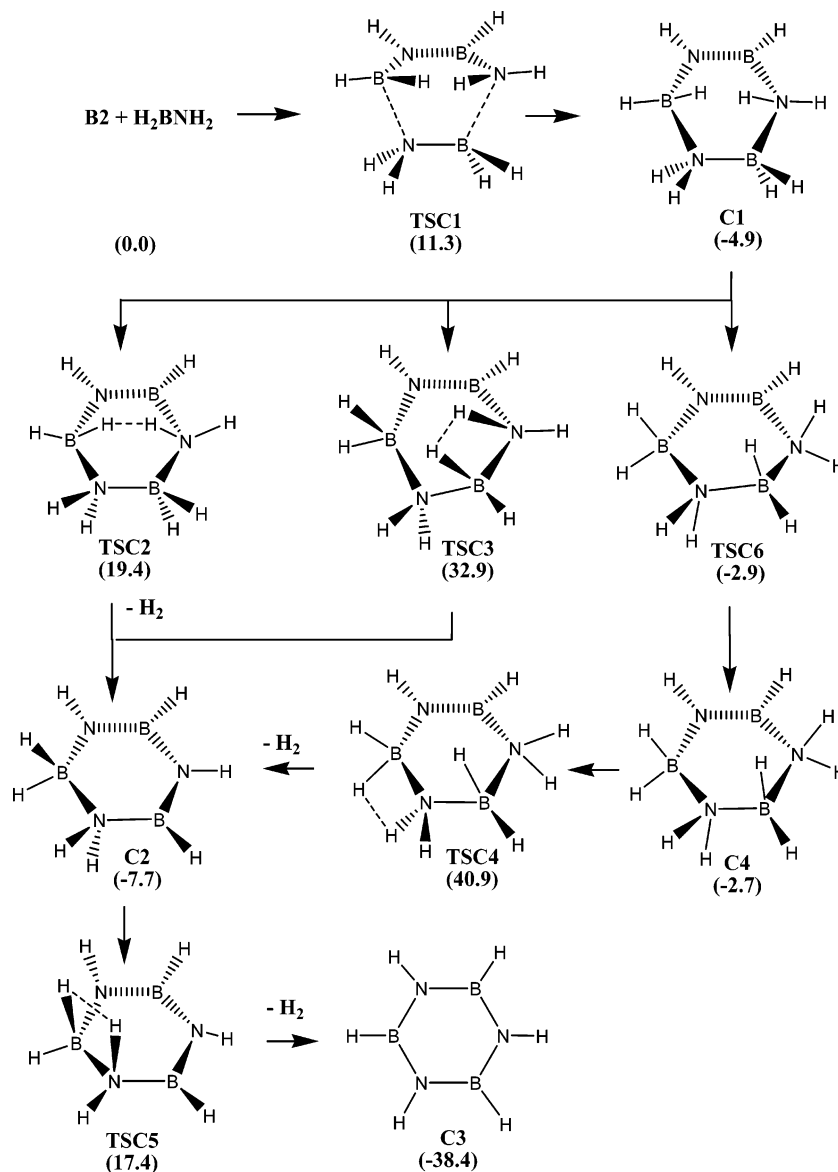


**Figure 3.** Potential-energy surface for the reaction of  $\mathbf{B2} + \mathbf{H2BNH2}$  in the cycloaddition pathway. Enthalpies (kcal/mol) are relative to  $\mathbf{B2} + \mathbf{H2BNH2}$  at 298.15 K.

**Table 4.** Relative Enthalpies (kcal/mol) and Free Energies (kcal/mol) at the B3LYP/6-311+G(2d,p)//B3LYP/6-31G(d) Level and 298.15 K

	$\Delta H$	$\Delta G$
$\mathbf{B2} + \mathbf{H2BNH2}$	0.0	0.0
<b>TSC1</b>	11.3	23.8
<b>C1</b>	-4.9	9.1
<b>TSC2</b>	19.4	34.2
<b>TSC3</b>	32.9	47.1
<b>TSC4</b>	40.9	54.8
$\mathbf{C2} + \mathbf{H2}$	-7.7	-2.4
$\mathbf{TSC5} + \mathbf{H2}$	17.4	23.0
$\mathbf{C3} + 2 \mathbf{H2}$	-38.4	-40.2
<b>TSC6</b>	-2.9	12.0
<b>C4</b>	-2.7	11.1

conformer (**D3**) of 1,3,5-triaza-2,4,6-triborahexatriene or the *cZc* conformer (**D6**). The enthalpy barrier (**TSD3**, 29.1 kcal/mol) to **D3** is slightly smaller than the barrier (**TSD8**, 31.8 kcal/mol) to **D6**. As with (*Z*)-hexatriene,<sup>33</sup> the *cZt* conformer

is more stable than the *cZc* form (4.2 kcal/mol), and the barriers to racemization (**TSD4**, 0.2; **TSD9**, 0.1 kcal/mol) are small. Rotation about the B(4)–N(5) bond in **D4** (**TSD5**, 7.6 kcal/mol) results in the *cZc* rotator (**D5**).

The disrotatory electrocycloization of **D5** (**TSD7**, 13.0 kcal/mol) leads to **C2**. However, the barrier height to **C2** via the conrotatory electrocyclic path (**TSD6**, 7.2 kcal/mol) is 5.8 kcal/mol lower. Whereas the electrocycloization of *cZc*-hexatriene is exothermic (–13.2 kcal/mol at the B3LYP/6-31(d,p) level and 298.15 K),<sup>33a</sup> the electrocyclic reaction of **D5** is slightly endothermic (0.9 kcal/mol) at 298.15 K and becomes slightly exothermic (–0.4 kcal/mol) at 573.15 K. Indeed, the *cZt* conformer (**D3**) is the most-stable species on this potential-energy surface (Figure 4). Also, it is noteworthy that the enthalpy barriers (6.3, 12.1 kcal/mol) for the reverse reactions (**C2**–**D5**) are significantly smaller than the barrier (**TSC5**, 25.1 kcal/mol) to (HBNH)<sub>3</sub> (**C3**).

At 573.15 K, the calculated free-energy barrier for **TSD1** (33.3 kcal/mol) is 10.7 kcal/mol higher than the value (22.6

(33) (a) Rodriguez-Otero, J. J. *Org. Chem.* **1999**, *64*, 6842. (b) Henseler, D.; Rebentisch, R.; Hohlneicher, G. *Int. J. Quantum Chem.* **1999**, *72*, 295.

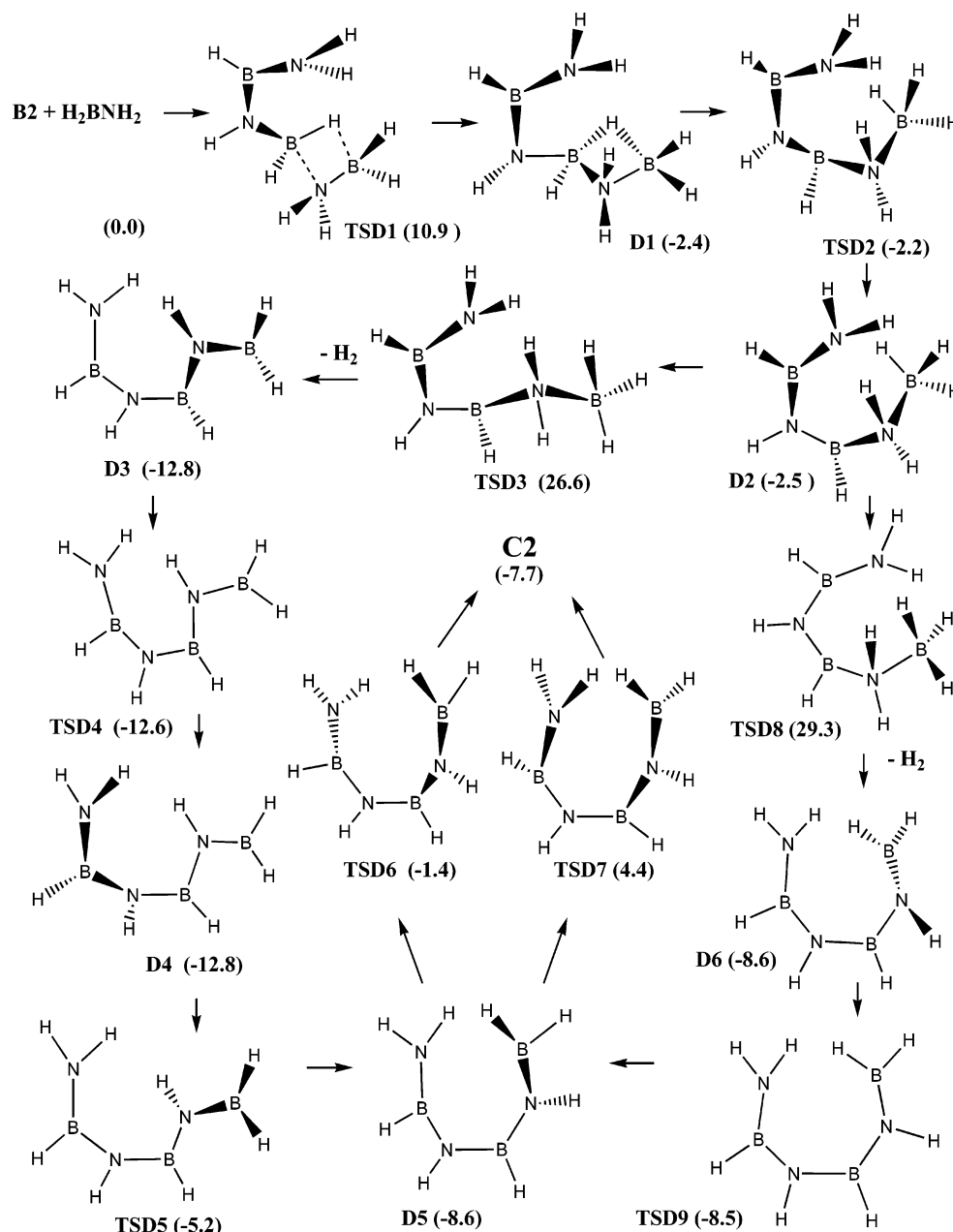


**Figure 4.** Potential-energy surface for the reaction of  $\text{B}_2 + \text{H}_2\text{BNH}_2$  in the electrocyclic pathway. Enthalpies (kcal/mol) are relative to  $\text{B}_2 + \text{H}_2\text{BNH}_2$  at 298.15 K.

kcal/mol) calculated at 298.15 K. The free-energy barrier heights of **TSD6** (9.4 kcal/mol) and **TSD7** (14.8 kcal/mol) exhibit much-smaller increases (2.1 and 2.0 kcal/mol), and the free-energy barriers (6.1, 11.5 kcal/mol) for the reactions in the reverse direction (**C2**–**D5**) decrease slightly (–0.3, –0.4 kcal/mol) over the same temperature range. The calculated barrier heights of **TSD3** (29.1 kcal/mol) and **TSD8** (31.9 kcal/mol) at 298.15 and 573.15 K differ by only 0.1 kcal/mol.

**Cyclotriborazane Pathway.** Cyclotriborazane,  $(\text{H}_2\text{BNH}_2)_3$ , is a known precursor to borazine. Dahl and Schaefer first reported<sup>34</sup> the formation of  $(\text{HBNH})_3$  from the thermolysis of  $(\text{H}_2\text{BNH}_2)_3$ . The pure solid is stable at temperatures below 150 °C. When a sample of  $(\text{H}_2\text{BNH}_2)_3$  was heated in a sealed

tube to 205 °C for 150 min,  $(\text{HBNH})_3$  was isolated in a 75% yield.<sup>34</sup> In 1988, Wang and Geanangel investigated<sup>35</sup> the thermal decomposition of  $\text{H}_3\text{BNH}_3$  in several aprotic solvents and at temperatures from 85 to 140 °C, with the aid of  $^{11}\text{B}$  NMR. The results of this study indicate that  $(\text{H}_2\text{BNH}_2)_3$  and/or  $(\text{H}_2\text{BNH}_2)_2$  (the chemical shifts of these two compounds were indistinguishable) were formed prior to the production of  $(\text{HBNH})_3$ . The concentrations of  $(\text{H}_2\text{BNH}_2)_3$  and/or  $(\text{H}_2\text{BNH}_2)_2$  grew and then decreased with an increase in the concentration of  $(\text{HBNH})_3$ . The authors were able to successfully isolate and characterized  $(\text{H}_2\text{BNH}_2)_3$  from the thermolysis reactions in diglyme. The rates of the formation of  $(\text{H}_2\text{BNH}_2)_3$  and  $(\text{HBNH})_3$  were found to be dependent on the nature of the solvent and the temperature.<sup>35</sup>

(34) Dahl, G. H.; Schaefer, R. *J. Am. Chem. Soc.* **1961**, *83*, 3032.

(35) Wang, J. S.; Geanangel, R. A. *Inorg. Chim. Acta* **1988**, *148*, 185.

**Table 5.** Relative Enthalpies (kcal/mol) and Free Energies (kcal/mol) at the B3LYP/6-311+G(2d,p)//B3LYP/6-31G(d) Level and 298.15 K

	$\Delta H$	$\Delta G$
<b>B2</b> + H <sub>2</sub> BNH <sub>2</sub>	0.0	0.0
<b>TSD1</b>	10.9	22.6
<b>D1</b>	-2.4	10.5
<b>TSD2</b>	-2.2	10.9
<b>D2</b>	-2.5	9.3
<b>TSD3</b>	26.6	38.4
<b>D3</b> + H <sub>2</sub>	-12.8	-9.6
<b>TSD4</b> + H <sub>2</sub>	-12.6	-8.8
<b>D4</b> + H <sub>2</sub>	-12.8	-9.6
<b>TSD5</b> + H <sub>2</sub>	-5.2	-1.4
<b>D5</b> + H <sub>2</sub>	-8.6	-5.7
<b>TSD6</b> + H <sub>2</sub>	-1.4	3.7
<b>TSD7</b> + H <sub>2</sub>	4.4	9.1
<b>TSD8</b>	29.3	41.2
<b>D6</b> + H <sub>2</sub>	-8.6	-5.7
<b>TSD9</b> + H <sub>2</sub>	-8.5	-4.6
<b>C2</b> + H <sub>2</sub>	-7.7	-2.4

The first step in the pathway (Figure 5) to (H<sub>2</sub>BNH<sub>2</sub>)<sub>3</sub> is the insertion of **B1** into the B–H bond of H<sub>2</sub>BNH<sub>2</sub> to form 1,3,5-triaza-2,4,6-triborahex-1-ene (**E1**). The calculated enthalpy barrier (**TSE1**, 12.1 kcal/mol) for this insertion reaction is similar in magnitude to barrier heights (**TSB1**, 11.4 kcal/mol; **TSD1**, 10.9 kcal/mol) calculated for the other insertion reactions. Rotation about the N(3)–B(4) bond in **E1** leads to a second conformer **E2**, which is less stable than **E1** by 1.3 kcal/mol (Table 6). The calculated enthalpy barrier height of **TSE2** is 1.6 kcal/mol. The continued clockwise rotation about the N(3)–B(4) bond in **E1** produces a third conformer **E3** that is the precursor to the cyclization step. **E3** is 0.1 kcal/mol less stable than **E2** and has a classical energy barrier (**TSE3**) of 0.3 kcal/mol. With the inclusion of the enthalpy correction, the calculated rotational barrier height (**TSE3**) is -0.4 kcal/mol. Only the free-energy barrier height for **TSE1** (23.6 kcal/mol) has a significant increase (10.5 kcal/mol) with an increase in the temperature from 298.15 to 573.15 K.

Cyclization of **E3** yields the chair conformation of (H<sub>2</sub>BNH<sub>2</sub>)<sub>3</sub> (**E4**). The calculated enthalpy barrier (**TSE4**) for the cyclization step is 27.8 kcal/mol. The transfer of a hydridic hydrogen atom from boron atom B(6) to boron atom B(2) in **E3** is nearly complete in transition state **TSE4**. The B–H bond lengths on B(2) in **TSE4** are 1.222 and 1.226 Å. The latter value is associated with the transferred hydrogen atom. The twisted conformation of (H<sub>2</sub>BNH<sub>2</sub>)<sub>3</sub> (**E5**, twist boat) is 0.4 kcal/mol more stable than the chair form at the B3LYP/6-311+G(2d,p)//B3LYP/6-31G(d) level and 1.1 kcal/mol more stable at the CCSD(T)/CBS level.<sup>21</sup> The enthalpy barrier height to conformational isomerization is 3.0 kcal/mol. In an earlier theoretical study, the eclipsed boat (*C<sub>s</sub>*) was found to be the most-stable conformer of (H<sub>2</sub>BNH<sub>2</sub>)<sub>3</sub>.<sup>36</sup> At the B3LYP/6-311+G(2d,p)//B3LYP/6-31G(d) level, this structure is the transition-state structure (**TSE8**) for the racemization of **E5** with a classical barrier height of 0.5 kcal/mol. The chair conformer (**E4**) was found to be the more-stable isomer in the solid state<sup>37</sup> and has been modeled at the B3LYP/6-311+G(d,p) level in a recent theoretical study of aromaticity.<sup>31a</sup>

In the final step, the **E5** conformer undergoes a 1,2-hydrogen elimination reaction and forms **C1** and molecular hydrogen. Two hydrogen-elimination pathways to **C1** were found. The pathway with the lower enthalpy barrier (48.8 kcal/mol) has a transition state (**TSE7**) in which the exiting hydrogens occupy pseudo-equatorial sites on a boron atom and a neighboring nitrogen atom. The boron atom lies on the C<sub>2</sub> axis in the **E5** conformer. The transition state (**TSE6**) for the second pathway is 2.5 kcal/mol higher in energy than the barrier height of **TSE7**, and the exiting hydrogen atoms occupy pseudoaxial sites.

**Triazatriborahexadiene Pathway.** This section examines possible pathways in which 1,3,5-triaza-2,4,6-triborahexa-1,5-diene is a precursor to (HBNH)<sub>3</sub>. The labels adopted by Gung et al.<sup>38b</sup> to identify the different conformations of 1,5-hexadiene are used. Structurally, the modeled conformers of 1,3,5-triaza-2,4,6-triborahexa-1,5-diene are qualitatively similar to the conformers of 1,5-hexadiene.<sup>38</sup> In general, the N(1)B(2)N(3)B(4) and N(3)B(4)N(5)B(6) dihedral angles are smaller and the N(3)–B(4) bond lengths are longer.

Two pathways to the **B** conformer (**F3**) of 1,3,5-triaza-2,4,6-triborahexa-1,5-diene from **E1** were investigated (Figure 6). Rotation about the B(3)–N(4) bond in **E1** leads to a more-stable conformation of 1,3,5-triaza-2,4,6-triborahex-1-ene (**F1**). The calculated classical barrier height (**TSF1**) to the rotation about the B(3)–N(4) bond in **E1** is 0.2 kcal/mol. The subsequent elimination of hydrogen from **F1** (**TSF2**, 41.1 kcal/mol) gives **F3** (Table 7). In an alternative pathway, **E1** eliminates hydrogen (**TSF3**, 39.9 kcal/mol) to produce the **E** conformer (**F2**). Rotation about the B(4)–N(5) bond in **F2**, for which the calculated classical barrier (**TSF4**) height is 0.4 kcal/mol, yields **F3**. The **A** (**F4**) and **E** (**F5**) conformers are achieved with rotation about the N(3)–B(4) and B(2)–N(3) bonds in **F3**. The calculated enthalpy barriers (**TSF5** and **TSF6**) to conformers **A** and **E** from **B** are 0.5 and 1.6 kcal/mol, respectively. **F5** is the enantiomer of **F2**. Rotation about the B(2)–N(3) bond in **A** (**TSF7**, 1.5 kcal/mol) leads to the **F** conformer (**F6**), and rotation about the N(3)–B(4) bond in **E** (**TSF12**, 0.5 kcal/mol) yields the **D** conformer (**F8**) (Figure 7).

The most-stable conformation of 1,3,5-triaza-2,4,6-triborahexa-1,5-diene is **B** (**F5**). The relative stabilities of the remaining conformers decrease in the order of **D**, **E**, **A**, **F**, and **J** (**F7**) at the B3LYP/6-311+G(2d,p)//B3LYP/6-31G(d) level. The difference in the enthalpy between conformers **B** and **D** is effectively zero (0.02 kcal/mol), and **B** is 2.5 kcal/mol more stable than the **J** conformer. A similar energetic ordering has been found for the conformers of 1,5-hexadiene.<sup>38</sup> However the **D** conformer of 1,5-hexadiene is the most stable at the MP2 level.<sup>38a</sup>

There are three reaction paths from the **F** conformer (**F6**) to (HBNH)<sub>3</sub> (Figure 7). In the lowest-energy pathway, rotation about the B(4)–N(5) bond in **F6** (**TSF9**, 0.8 kcal/mol) leads to the **J** conformer (**F7**), and, subsequently, the

(36) Findlay, R. H. *J. Chem. Soc., Dalton Trans* **1976**, 851.(37) Corfield, P. W. R.; Shore, S. G. *J. Am. Chem. Soc.* **1973**, *95*, 1480.(38) (a) Rocque, B. G.; Gonzales, J. M.; Schaefer, H. F., III *Mol. Phys.* **2002**, *100*, 441. (b) Gung, B. W.; Zhu, Z.; Fouch, R. A. *J. Am. Chem. Soc.* **1995**, *117*, 1783.



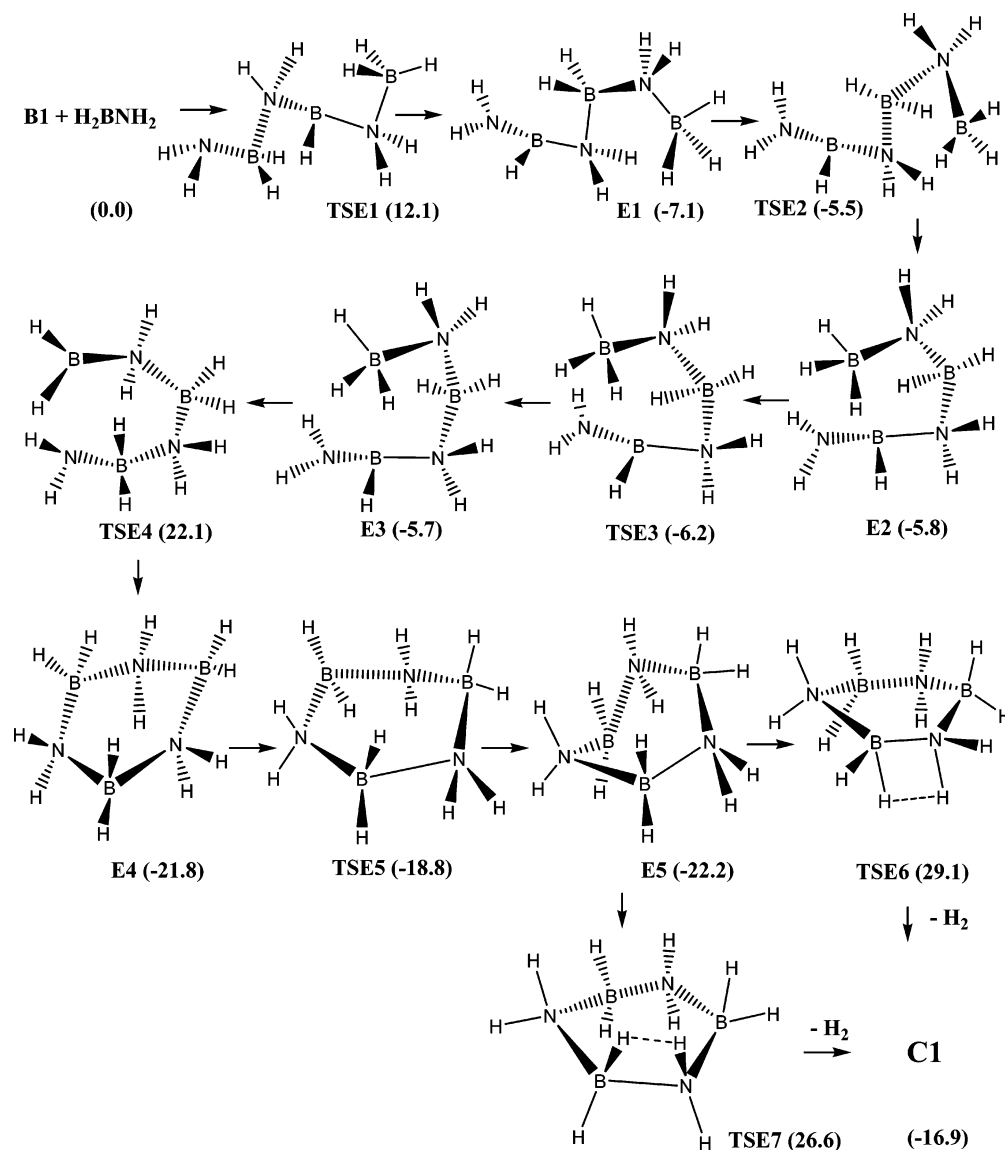


**Figure 5.** Potential-energy surface for the reaction of **B1** +  $\text{H}_2\text{BNH}_2$  in the cyclotriborazane pathway. Enthalpies (kcal/mol) are relative to **B1** +  $\text{H}_2\text{BNH}_2$  at 298.15 K.

**Table 6.** Relative Enthalpies (kcal/mol) and Free Energies (kcal/mol) at the B3LYP/6-311+G(2d,p)//B3LYP/6-31G(d) Level and 298.15 K

	$\Delta H$	$\Delta G$
<b>B1</b> + $\text{H}_2\text{BNH}_2$	0.0	0.0
<b>TSE1</b>	12.1	23.6
<b>E1</b>	-7.1	4.5
<b>TSE2</b>	-5.5	7.9
<b>E2</b>	-5.8	6.8
<b>TSE3</b>	-6.2	7.8
<b>E3</b>	-5.7	7.3
<b>TSE4</b>	22.1	36.3
<b>E4</b>	-21.8	-6.3
<b>TSE5</b>	-18.8	-3.5
<b>E5</b>	-22.2	-7.2
<b>TSE6</b>	29.1	43.9
<b>TSE7</b>	26.6	41.4
<b>C1</b> + $\text{H}_2$	-16.9	-10.9
<b>TSE8</b>	-22.2	-6.5

cyclization of **F7** (**TSF10**, 15.5 kcal/mol) yields **C1**. Rotation about the **N(3)**–**B(4)** bond in **F6** (**TSF8**, 0.4 kcal/mol) gives the **D** conformer (**F8**) in the second path. The unimolecular elimination of  $\text{H}_2$  from **F8** (**TSF13**, 29.3 kcal/mol) produces the most-stable conformation of 1,3,5-triaza-2,4,6-tribora-

hexatriene, the *tZt*<sup>32</sup> conformer (**F9**). The calculated enthalpy barrier (**TSF14**) to the *cZt* conformer (**D4**) via rotation about the **B(2)**–**N(3)** bond in **F9** is 9.4 kcal/mol. The third pathway involves the elimination of  $\text{H}_2$  by **F6** (**TSF11**, 29.1 kcal/mol) to form the *cZc* conformer (**D5**).

The free-energy barriers (**TSF2** and **TSF3**) to the elimination of  $\text{H}_2$  from **F1** and **E1** are 39.8 and 39.6 kcal/mol respectively at 298.15 K and 38.5 and 39.2 kcal/mol respectively at 573.15 K. The increases of 1.0, 0.6, and 0.7 kcal/mol in the free-energy barrier heights of **TSF11** (30.0 kcal/mol), **TSF13** (29.8 kcal/mol), and **TSF14** (10.0 kcal/mol) with an increase temperature from 298.15 to 573.15 K are also small. The calculated free-energy barrier for **TSF10** (21.0 kcal/mol) at 573.15 K is 2.8 kcal/mol higher than the value (18.2 kcal/mol) calculated at 298.15 K.

**Comparison of the B3LYP/6-311+G(2d,p)//B3LYP/6-31G(d) Method with Higher Levels of Theory.** Dixon and co-workers have calculated the enthalpy changes ( $\Delta H(298\text{ K})$ ) in a variety of condensation and hydrogen-elimination

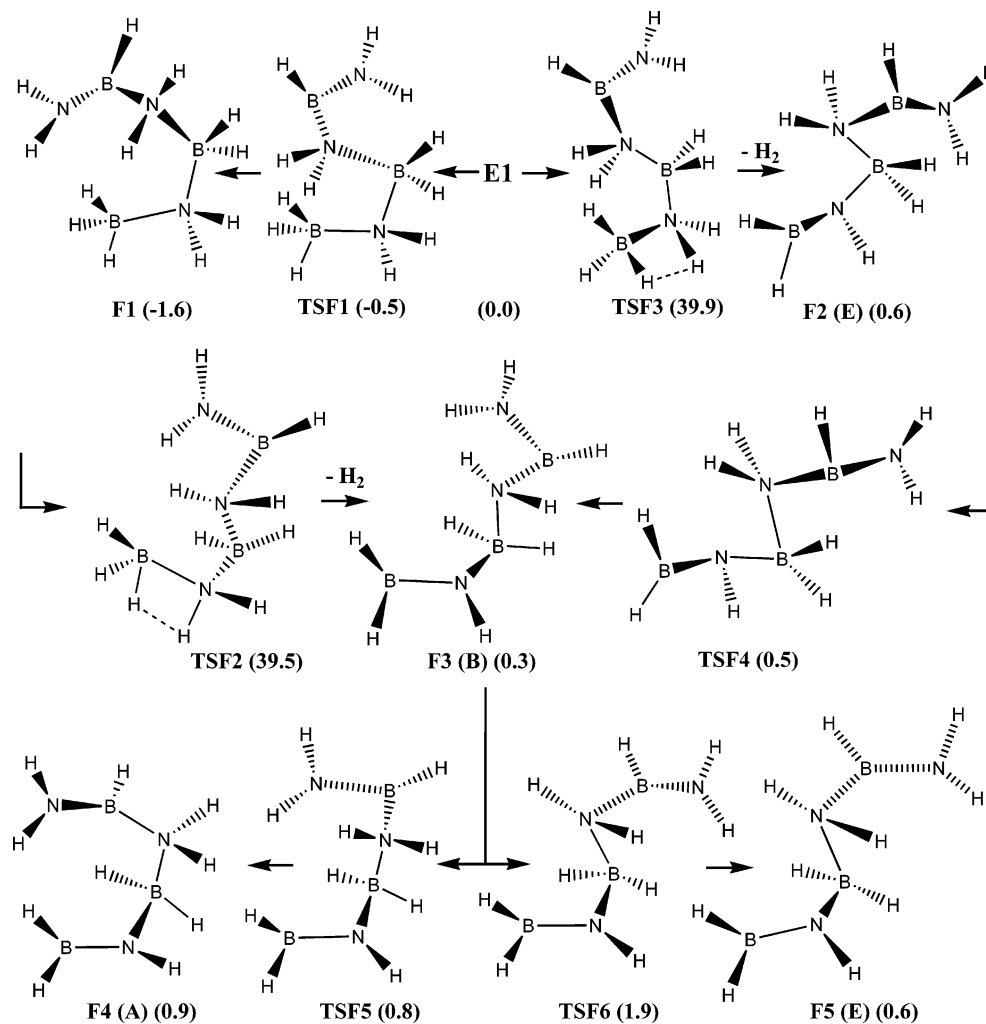


**Figure 6.** Potential-energy surface for the reaction of **E1** in the triazatriborahexadiene pathway. Enthalpies (kcal/mol) are relative to **E1** at 298.15 K.

reactions of boron–nitrogen compounds at both the CCSD(T)/CBS and B3LYP/6-311+G(d,p) levels.<sup>21</sup> The root mean square (rms) deviation of the reaction enthalpies calculated at the latter level from the reaction enthalpies calculated at the former level is 7.3 kcal/mol, and the maximum deviation in the set of 34 reactions studied is 18.4 kcal/mol. A comparison of seven reaction enthalpies calculated at the B3LYP/6-311+G(2d,p)//B3LYP/6-31G(d) level with values obtained from the CCSD(T)/CBS<sup>18,21</sup> calculated enthalpies of formation is found in Table S8 of the Supporting Information. The rms deviation of the values calculated at the B3LYP/6-311+G(2d,p)//B3LYP/6-31G(d) level from the values obtained at higher levels of theory is 3.9 kcal/mol, and the maximum deviation is 6.2 kcal/mol.

The agreement between the energy barriers calculated at the B3LYP/6-311+G(2d,p)//B3LYP/6-31G(d) level and at higher levels of theory is better. Table 8 contains six barrier heights ( $\Delta H(0\text{ K})$ ) calculated at the B3LYP/6-311+G(2d,p)//B3LYP/6-31G(d) and CCSD(T)/aVTZ<sup>18,39</sup> levels. The rms deviation of the barrier heights calculated at the B3LYP/6-311+G(2d,p)//B3LYP/6-31G(d) level from the barrier heights calculated at the CCSD(T)/aVTZ level is 2.4 kcal/mol, and

**Table 7.** Relative Enthalpies (kcal/mol) and Free Energies (kcal/mol) at the B3LYP/6-311+G(2d,p)//B3LYP/6-31G(d) Level and 298.15 K

	$\Delta H$	$\Delta G$
<b>E1</b>	0.0	0.0
<b>TSF1</b>	-0.5	0.8
<b>F1</b>	-1.6	-0.6
<b>TSF2</b>	39.5	39.2
<b>TSF3</b>	39.9	39.6
<b>F2 + H<sub>2</sub></b>	0.6	-8.6
<b>TSF4 + H<sub>2</sub></b>	0.5	-7.4
<b>F3 + H<sub>2</sub></b>	0.3	-9.0
<b>TSF5 + H<sub>2</sub></b>	0.8	-7.0
<b>F4 + H<sub>2</sub></b>	0.9	-7.6
<b>TSF6 + H<sub>2</sub></b>	1.9	-5.9
<b>F5 + H<sub>2</sub></b>	0.6	-8.6
<b>TSF7 + H<sub>2</sub></b>	2.4	-4.6
<b>F6 + H<sub>2</sub></b>	1.8	-7.0
<b>TSF8 + H<sub>2</sub></b>	2.2	-5.6
<b>TSF9 + H<sub>2</sub></b>	2.6	-4.5
<b>F7 + H<sub>2</sub></b>	2.8	-5.2
<b>F8 + H<sub>2</sub></b>	0.3	-8.4
<b>TSF10 + H<sub>2</sub></b>	18.3	13.0
<b>C1 + H<sub>2</sub></b>	-9.8	-15.4
<b>TSF11 + H<sub>2</sub></b>	30.9	23.0
<b>D5 + 2 H<sub>2</sub></b>	-13.5	-30.2
<b>TSF12 + H<sub>2</sub></b>	1.1	-6.5
<b>TSF13 + H<sub>2</sub></b>	29.6	21.4
<b>F9 + 2 H<sub>2</sub></b>	-20.6	-37.2
<b>TSF14 + 2 H<sub>2</sub></b>	-11.2	-27.2
<b>D4 + 2 H<sub>2</sub></b>	-17.7	-34.1

(39) Nguyen, V. S.; Matus, M. H.; Grant, D. J.; Nguyen, M. T.; Dixon, D. *A. J. Phys. Chem. A* **2007**, ASAP.

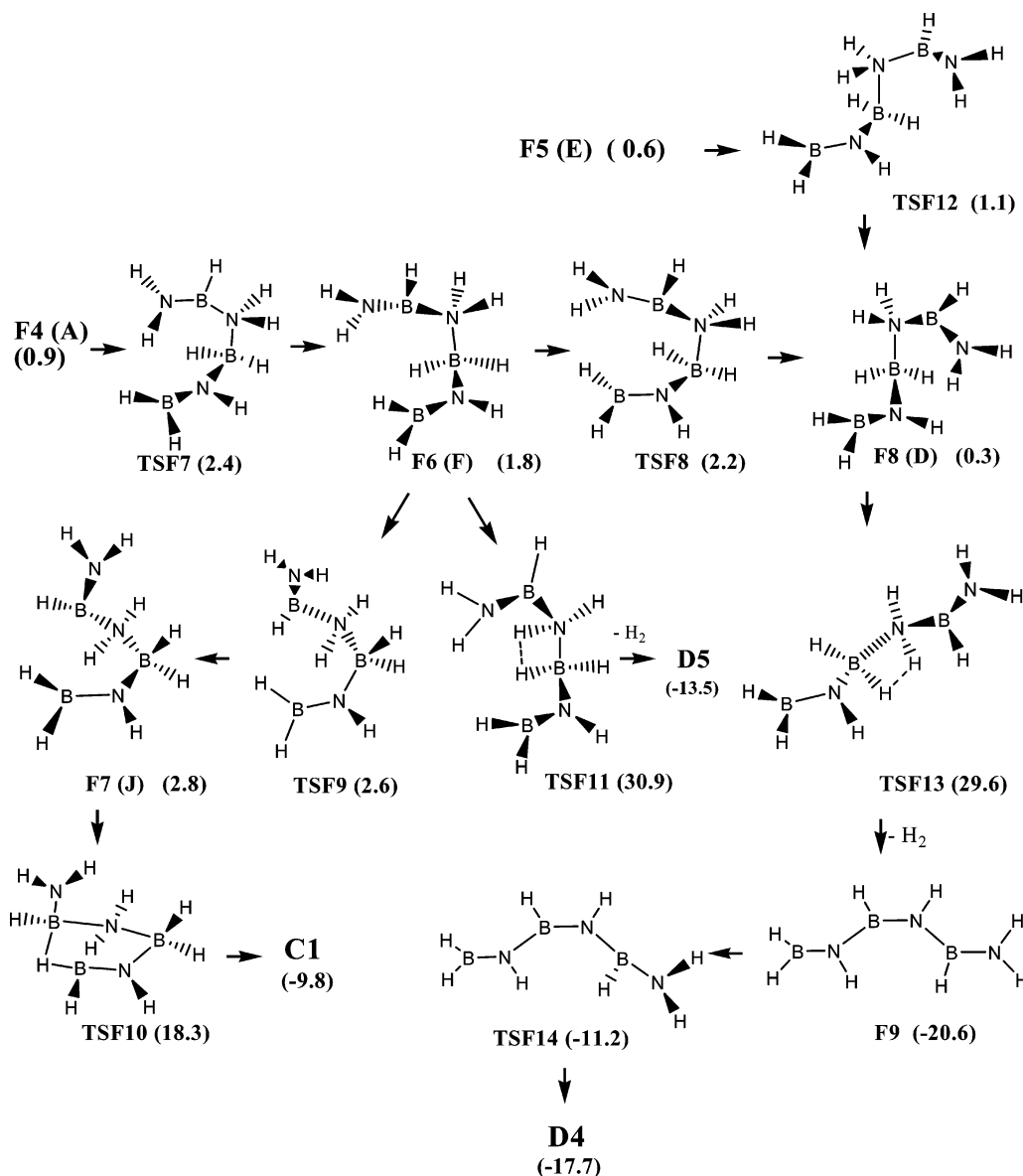


**Figure 7.** Potential-energy surface for the reaction of **E1** in the triazatriborahexadiene pathway continued. Enthalpies (kcal/mol) are relative to **E1** at 298.15 K.

**Table 8.** A Comparison of Barrier Heights (kcal/mol) Calculated at B3LYP/6-311+G(2d,p)//B3LYP/6-31G(d) and CCSD(T)/aVTZ Levels

reaction	$\Delta H(0K)^a$	$\Delta H(0K)$
<b>1</b> $\rightarrow$ <b>TS2</b> $\rightarrow$ $H_2BNH_2 + H_2 + BH_3$	20.2	24.1 <sup>b</sup>
$H_3BNH_3 \rightarrow$ <b>TS4</b> $\rightarrow$ $H_2BNH_2 + H_2$	34.3	36.8 <sup>b</sup>
<b>A3</b> $\rightarrow$ <b>TSA5</b> $\rightarrow$ <b>A2</b>	1.6	2.0 <sup>c</sup>
$2 H_3BNH_3 \rightarrow$ <b>TS6</b> $\rightarrow$ $2 H_2BNH_2 + 2 H_2$	34.4	36.0 <sup>c</sup>
$2 H_3BNH_3 \rightarrow$ <b>TS7</b> $\rightarrow$ $H_3BNH_3 + H_2BNH_2 + H_2$	34.7	33.9 <sup>c</sup>
$[(H_3N)_2BH_2][BH_4](3) \rightarrow$ <b>TS8</b> $\rightarrow$ <b>2</b> + $BH_3 + H_2$	17.3	20.5 <sup>c</sup>

<sup>a</sup> Calculated at the B3LYP/6-311+G(2d,p)//B3LYP/6-31G(d) level with inclusion of the zero-point energy. <sup>b</sup> Calculated at the CCSD(T)/aVTZ level with inclusion of the zero-point energy, ref 18. <sup>c</sup> Calculated at the CCSD(T)/aVTZ level with inclusion of the zero-point energy, ref 39.

the maximum deviation is 3.9 kcal/mol. Similar deviations in the barriers heights calculated at the B3LYP/6-311++G-(d,p) and G3 levels have been found for the pericyclic reactions of  $H_2BNH_2$  with  $H_2BNH_2$ ,  $H_2CCH_2$ , or  $H_2CCHCH_3$ .<sup>40</sup> The rms and maximum deviations are 3.2 and

4.4 kcal/mol, respectively. Barrier heights calculated at the B3LYP/6-311+G(2d,p)//B3LYP/6-31G(d) level are predicted to deviated from values obtained at higher levels of theory by  $\pm 3$  kcal/mol.

**Calculated Rate Constants.** Intermediate **B1** is a reactant in both a bimolecular,  $B1 + H_2BNH_2 \rightarrow E1$ , and unimolecular,  $B1 \rightarrow B2 + H_2$ , reaction, and the free-energy barrier heights of **TSE1** and **TSB3** differ by only 3.5 kcal/mol. In an effort to identify the kinetically preferred path, the rate constants were calculated for the two reactions. The calculations were performed with the TheRate program<sup>41</sup> and at the TST and at the TST with the Eckart tunneling correction<sup>42</sup> levels. The calculated rate constants with the Eckart tunneling correction are  $9.4 \times 10^{-4}$  and  $6.0 \times 10^{-1}$  M/sec respectively for the bimolecular reaction and  $2.6 \times 10^{-6}$  and  $5.7 \times 10^{-2}$  sec<sup>-1</sup> respectively for the unimolecular reaction at 298 and

(41) Zhang, S.; Truong, T. N. *VKLab* version 1.0, University of Utah: Salt Lake City, UT, 2001.

(42) Truong, T. N.; Truhlar, D. G. *J. Chem. Phys.* **1990**, *93*, 1761.

(40) Bissett, K. M.; Gilbert, T. M. *Organometallics* **2004**, *23*, 850.

573 K. Tables of the calculated rate constants for the bimolecular and unimolecular reactions in this study are included in the Supporting Information (Table S6 and Table S7).

In the first synthesis of (HBNH)<sub>3</sub> by Stock and Pohland,<sup>3</sup> the initial concentrations of B<sub>2</sub>H<sub>6</sub> and NH<sub>3</sub> were  $1.22 \times 10^{-3}$  and  $1.06 \times 10^{-2}$  M, respectively, in one experiment. If it is assumed for the purpose of this computation that all of the B<sub>2</sub>H<sub>6</sub> is converted to H<sub>2</sub>BNH<sub>2</sub>, then an upper range of concentrations for **B1** and H<sub>2</sub>BNH<sub>2</sub> and the rates of the bimolecular and unimolecular reactions can be calculated. At 298 K, the calculated rates of the bimolecular and unimolecular reactions are  $1.1 \times 10^{-10}$  and  $1.3 \times 10^{-10}$  M/sec respectively when the concentrations of **B1** and H<sub>2</sub>BNH<sub>2</sub> are  $5.0 \times 10^{-5}$  and  $2.3 \times 10^{-3}$  M, and  $4.1 \times 10^{-10}$  and  $2.6 \times 10^{-9}$  M/sec respectively when the concentrations are  $1.0 \times 10^{-3}$  and  $4.4 \times 10^{-4}$  M. The bimolecular and unimolecular reactions are predicted to have nearly the same rates when the concentrations of **B1** and H<sub>2</sub>BNH<sub>2</sub> are  $5.0 \times 10^{-5}$  and  $2.3 \times 10^{-3}$  M, but the rate of the unimolecular reaction will be 6.3 times faster at higher concentrations of **B1** and lower concentrations of H<sub>2</sub>BNH<sub>2</sub>. At 573 K, the rate of the unimolecular reaction, **B1** → **B2** + H<sub>2</sub>, is predicted to be at least 3 orders of magnitude faster than the rate of the bimolecular reaction, **B1** + H<sub>2</sub>BNH<sub>2</sub> → **E1**. The calculated rates of the bimolecular and unimolecular reactions are  $7.0 \times 10^{-6}$  and  $2.8 \times 10^{-2}$  M/sec respectively when the concentrations of **B1** and H<sub>2</sub>BNH<sub>2</sub> are  $5.0 \times 10^{-5}$  and  $2.3 \times 10^{-3}$  M, and  $2.6 \times 10^{-9}$  and  $5.7 \times 10^{-1}$  M/sec respectively at concentrations of  $1.0 \times 10^{-3}$  and  $4.4 \times 10^{-4}$  M for **B1** and H<sub>2</sub>BNH<sub>2</sub>.

## Conclusions

In this and earlier studies,<sup>10,11</sup> the pathway from B<sub>2</sub>H<sub>6</sub> and NH<sub>3</sub> to H<sub>2</sub>BNH<sub>2</sub> with the lowest free-energy barrier is B<sub>2</sub>H<sub>6</sub> + NH<sub>3</sub> → **TS1** → **1** → **TS2** → H<sub>2</sub>BNH<sub>2</sub> + BH<sub>3</sub> + H<sub>2</sub>. The unimolecular elimination of H<sub>2</sub> from H<sub>3</sub>BNH<sub>3</sub> (eq 8) has a calculated free-energy barrier height (**TS4**, 33.8 kcal/mol) that is 13.0 kcal/mol higher than barrier height of **TS2** (20.8 kcal/mol) at 298.15 K, and the difference between the barrier heights of **TS4** (33.5 kcal/mol) and **TS2** (21.7 kcal/mol) is 11.8 kcal/mol at 573.15 K. The more facile pathway from H<sub>3</sub>BNH<sub>3</sub> to H<sub>2</sub>BNH<sub>2</sub> in the gas phase is 2 H<sub>3</sub>BNH<sub>3</sub> → **TS5** → **1** + NH<sub>3</sub>; **1** → **TS2** → H<sub>2</sub>BNH<sub>2</sub> + BH<sub>3</sub> + H<sub>2</sub>. Transition state **TS5** has a calculated free-energy barrier of 21.0 kcal/mol at 298.15 K and 26.6 kcal/mol at 573.15 K.

The reaction of NH<sub>3</sub> and B<sub>2</sub>H<sub>5</sub>NH<sub>2</sub> also affords a route to H<sub>2</sub>BNH<sub>2</sub> (Figure 1). The free-energy barrier (**TSA3**, 23.3 kcal/mol) in the lowest-energy path on this potential-energy surface, **A1** + NH<sub>3</sub> → **TSA4** → **A3** → **TSA5** → **A2** → **TSA3** → 2 H<sub>2</sub>BNH<sub>2</sub>, is 2.5 kcal/mol higher than the barrier (**TS2**, 20.8 kcal/mol) in the pathway (eqs 2 and 3) from B<sub>2</sub>H<sub>6</sub> and NH<sub>3</sub> to H<sub>2</sub>BNH<sub>2</sub> at 298.15 K. At 573.15 K, the barrier height of **TSA3** decreases to 22.2 kcal/mol, but the free-energy barrier (**TSA4**) to the formation of **A3** increases to 24.9 kcal/mol. The free-energy barrier (**TSA2**, 23.2 kcal/mol) in the alternative path from **A1** to **A2** increases to 28.4 kcal/mol at 573.15 K.

Insertion of H<sub>2</sub>BNH<sub>2</sub> into the B–H bond of a second H<sub>2</sub>BNH<sub>2</sub> to form **B1** has a free-energy barrier (**TSB1**) of 22.2 kcal/mol at 298.15 K and is the gateway step from H<sub>2</sub>BNH<sub>2</sub> to (HBNH)<sub>3</sub> in this study. In turn, **B1** may insert into the B–H bond of H<sub>2</sub>BNH<sub>2</sub> to form **E1**, and the free-energy barrier height (**TSE1**) to the formation of **E1** is 23.6 kcal/mol (Figure 5). Elimination of H<sub>2</sub> from **E1** (**TSF2**, 39.8 kcal/mol; **TSF3**, 39.6 kcal/mol) leads to **F3** and eventually to (HBNH)<sub>3</sub> via **C1**, **D4**, or **D5** (Figures 6 and 7). Cyclization (**TSE4**, 29.0 kcal/mol) of a conformer of **E1** to form (H<sub>2</sub>BNH<sub>2</sub>)<sub>3</sub> (**E4**) affords an alternative pathway to **C1** (Figure 5). However, the free-energy barriers to the elimination of H<sub>2</sub> from **E5** (**TSE6**, 51.1 kcal/mol and **TSE7**, 48.6 kcal/mol) and the formation of **C1** are also high.

1,3-diaza-2,4-diborabutene (**B1**) may also eliminate H<sub>2</sub>, for which the calculated free-energy barrier (**TSB3**) is 27.1 kcal/mol at 298.15 K, and form **B2** (Figure 2). Although the calculated free-energy barrier (**TSE1**, 23.6 kcal/mol) to the formation of the **E1** is 3.5 kcal/mol lower than the calculated free-energy barrier height of **TSB3**, the calculated rates of the formation of **E1** and **B2** are nearly the same ( $1.1 \times 10^{-10}$  and  $1.3 \times 10^{-10}$  M/sec, respectively) at low concentrations of **B1** ( $5.0 \times 10^{-5}$  M) and high concentrations of H<sub>2</sub>BNH<sub>2</sub> ( $2.3 \times 10^{-3}$  M). When the concentration of **B1** is high ( $1.0 \times 10^{-3}$  M) and the concentration of H<sub>2</sub>BNH<sub>2</sub> is low ( $4.4 \times 10^{-4}$  M), the calculated rate of formation of **B2** ( $2.6 \times 10^{-9}$  M/sec) is 6.3 times faster than the calculated rate of formation of **E1** ( $4.1 \times 10^{-10}$  M/sec). At 573.15 K, the predicted free-energy barrier height of **TSE1** (34.1 kcal/mol) exceeds the barrier height of **TSB3** (27.9 kcal/mol), and the calculated rate of formation of **B2** is at least 3 orders of magnitude faster than the rate of formation of **E1**. **B2** is predicted to be the favored product except at low concentrations of **B1**, high concentrations of H<sub>2</sub>BNH<sub>2</sub>, and a temperature of 298.15 K. Under these conditions, the rate of formation of **E1** is expected to be competitive with the rate of formation of **B2**, and the rate of formation of polyolefin **G1** is predicted to be at least 2 orders of magnitude faster than the rate of cyclization of **E3**.

**B2** may undergo either a cycloaddition reaction with H<sub>2</sub>BNH<sub>2</sub> to form **C1** or an insertion reaction with H<sub>2</sub>BNH<sub>2</sub> to produce **D1**. The calculated free-energy barrier heights for the former reaction (**TSC1**) are 23.8 and 35.3 kcal/mol respectively and for the latter reaction (**TSD1**) are 22.6 and 33.3 kcal/mol respectively at 298.15 and 573.15 K. The calculated rate constant with the Eckart tunneling correction for the latter reaction ( $5.2 \times 10^{-3}$  M/sec) is nearly eight times larger than the rate constant ( $6.4 \times 10^{-4}$  M/sec) for the former reaction at 298.15 K. At 573.15 K, the calculated rate constant for the latter reaction ( $1.2 \times 10^{+2}$  M/sec) is nearly six times larger than the calculated rate constant for the former reaction ( $2.1 \times 10^{+1}$  M/sec). At the B3LYP/6-311+G(2d,p)//B3LYP/6-31G(d) level of theory, it is not possible to predict which of the two pathways, the electrocyclic pathway: **B2** + H<sub>2</sub>BNH<sub>2</sub> → **TSD1** → **D1** → **D2** → **TSD3** → **D3** + H<sub>2</sub>; **D3** → **D4** → **TSD5** → **D5** → **TSD6** → **C2**; **C2** → **TSC5** → (HBNH)<sub>3</sub> + H<sub>2</sub> or the cycloaddition pathway: **B2** + H<sub>2</sub>BNH<sub>2</sub> → **TSC1** → **C1** → **TSC2** → **C2**

### *Theoretical Study of Reaction Pathways to Borazine*

+ H<sub>2</sub>; **C2** → **TSC5** → (HBNH)<sub>3</sub> + H<sub>2</sub>, is the more facile route to (HBNH)<sub>3</sub> in the gas phase. The cyclotriborazane and triazatriborahexadiene pathways contain steps with significantly larger calculated free-energy barriers and smaller rate constants and are less favorable than the cycloaddition and electrocyclic pathways to (HBNH)<sub>3</sub>.

**Supporting Information Available:** Table S1, total energies (hartrees), zero-point energies (kcal/mol), thermal corrections (kcal/mol), and entropies (cal/mol·K); Table S2, some barrier enthalpies and free energies at the B3LYP/6-311+G(2d,p)//B3LYP/6-31G(d) level and 573.15 K; Table S3, dihedral angles for some conformers of 1,3,5-triaza-2,4,6-triborahexa-1,5-diene; Table S4, some enthalpy and free-energy barriers arranged in order of

increasing magnitude; Table S5, Cartesian coordinates of geometries optimized at the B3LYP/6-31G(d) level; Table S6, bimolecular rate constants (M·sec<sup>-1</sup>) calculated with the conventional TST method and the TST method with Eckart tunneling correction and arranged in order of decreasing magnitude; Table S7, unimolecular rate constants (sec<sup>-1</sup>) calculated with the conventional TST method and the TST method with Eckart tunneling correction and arranged in order of decreasing magnitude; Table S8, a comparison of reaction enthalpies and free energies (kcal/mol) calculated at the B3LYP/6-311+G(2d,p)//B3LYP/6-31G(d) and CCSD(T)/CBS levels and at 298.15 K; Figure S1, molecular plots. This material is available free of charge via the Internet at <http://pubs.acs.org>.

IC070193S